

Time-dependent density-functional study of field emission from tipped carbon nanotubes

J. A. Driscoll and K. Varga

Department of Physics and Astronomy, Vanderbilt University, Nashville, Tennessee 37235, USA

(Received 19 August 2009; revised manuscript received 22 October 2009; published 22 December 2009)

Field emission from carbon nanotubes is studied by propagating the electronic wave function in real time using time-dependent density-functional theory. Complex absorbing potentials have been employed to avoid artificial reflections from the boundaries and to allow long time simulations. Domain decomposition is used to facilitate accurate and efficient wave function propagation. The influence of adsorbed atoms on field emission is investigated. It is found that adsorbate atoms significantly increase the field-emission current and cause strong differences and nonlinearity in the Fowler-Nordheim plot.

DOI: [10.1103/PhysRevB.80.245431](https://doi.org/10.1103/PhysRevB.80.245431)

PACS number(s): 73.63.Fg, 71.15.Mb

I. INTRODUCTION

Field emission (FE) from nanostructures is the subject of intense experimental and theoretical research. The aim of these studies is to explore the properties of nanoscale materials in intense electric fields and exploit these properties for technological applications. Emission from carbon nanotubes (CNs) is particularly important as CNs are candidates for next-generation displays, electron sources,¹⁻⁴ and high-resolution electron beam instruments.⁵⁻⁸

The intensity, spatial and energy resolution, and other properties of the electron beam depend on the electronic structure of the field emitter. Structural defects, adsorbates, encapsulated atoms, and other variations in the atomic structure significantly change the FE properties of CNs. Experimental studies investigating the effects of adsorbates on field emission have shown that adsorbates strongly influence the field-emission current.⁹⁻¹⁴ For example, experiments have shown that a Cs adsorbate can significantly increase the FE current.^{15,16} Other adsorbates, e.g., CH₄ and CO molecules can increase or decrease the field-emission current.^{13,14} To understand the key physical processes determining the FE properties, it is highly desirable to have a first-principles description of the emitted current in terms of the electronic structure of realistic materials subject to an electric field.

In this paper, the field emission of carbon nanotubes is investigated by using time-dependent density-functional theory (TDDFT).¹⁷ To simulate field emission, the wave functions of the electrons are propagated in real space and real time. Systems with different adsorbed atoms are investigated to study the effect of adsorbed atoms on the field-emission current. The calculations show that the field emission is significantly enhanced due to adsorbed atoms. The adsorbates introduce additional electron orbitals, which are localized around the tip of the nanotube and electrons are easily emitted from these states.

The theoretical study of field emission dates back to the early days of quantum mechanics. The standard approach to modeling field emission is the Fowler-Nordheim (FN) theory,¹⁸ which describes the emission of electrons from a flat metal surface in the presence of an electric field. More rigorous methods that take into account atomic geometry and electronic structure have been developed in the last few years¹⁹⁻²² including first-principles calculations. The first-

principles approaches calculate the self-consistent electronic structure of the field emitter and connect the wave function to the asymptotic scattering wave function of the electrons in the external field.^{20,21} An important step beyond the static calculations is the introduction of the time-dependent description of FE.^{23,24} The time-dependent description so far has been limited to time propagation of the wave functions with a time-independent ground state Hamiltonian.

The present work goes beyond previous time-dependent approaches^{23,24} and simulates the entire field-emission process in a real time, real space framework. In the time-dependent approach, the wave function is time propagated to describe the effect of the electric field. This approach has several advantages. In the time-independent approach, the wave function has to be matched to the asymptotic wave function. The asymptotic wave function, the wave function of electrons in an electric field, is not known. It is usually approximated by Airy functions, the wave functions of independent, noninteracting electrons in an electric field. This approximation is avoided in the time-dependent approach: the field-emitted electrons and the electrons of the nanotube are described on an equal footing. The asymptotic form of the wave function is not needed in the calculation, and the time evolution of the wave function is used to describe the emitted current.

II. FORMALISM

In the TDDFT framework,¹⁷ the electronic motion is described by the following time-dependent Kohn-Sham equation for single particle orbitals Ψ_i :

$$i\hbar \frac{\partial}{\partial t} \Psi_i(\mathbf{r}, t) = H \Psi_i(\mathbf{r}, t) \quad (1)$$

with

$$H = H_{KS} + V_{ext} \quad (2)$$

$$H_{KS} = -\frac{\hbar^2}{2m} \nabla_{\mathbf{r}}^2 + V_A(\mathbf{r}, t) + V_H(\mathbf{r}, t) + V_{XC}[\rho](\mathbf{r}, t), \quad (3)$$

where $V_{ext}(\mathbf{r}, t)$ is the time-dependent external potential, $V_A(\mathbf{r}, t)$ is the atomic potential, $V_H(\mathbf{r}, t)$ is the Hartree potential, and $V_{XC}(\mathbf{r}, t)$ is the exchange-correlation potential. The

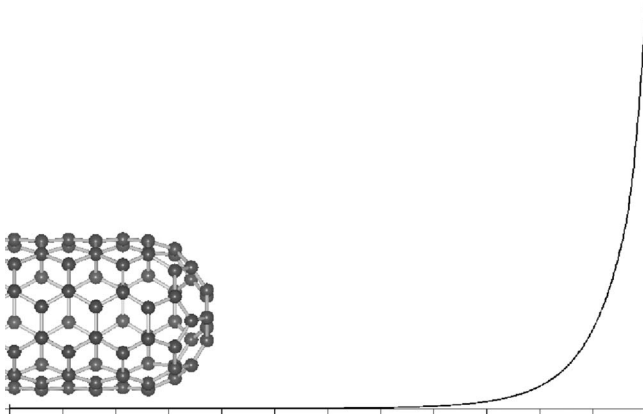


FIG. 1. Use of a complex potential in a field-emission calculation. The vertical lines indicate the measurement region for electron density. The imaginary potential absorbs the wave function in the asymptotic region, preventing reflections.

pseudopotential approach²⁵ is used to represent the atomic potentials $V_A(\mathbf{r}, t)$. The exchange-correlation potential $V_{XC}(\mathbf{r}, t)$ is constructed using the adiabatic local density approximation²⁶ and the Hartree potential is calculated by solving the Poisson equation. The electron charge density is given by $\rho(\mathbf{r}, t) = \sum_i |\Psi_i(\mathbf{r}, t)|^2$ and the current is defined as

$$\mathbf{j}(\mathbf{r}, t) = \frac{e\hbar}{2im} \sum_i (\Psi_i^* \nabla \Psi_i - \Psi_i \nabla \Psi_i^*). \quad (4)$$

One difficulty in time-dependent calculations arises from the finite size of the simulation volume. Typically, long simulation times are needed for the system to reach a steady state in which measurements can be made. In a finite simulation volume, however, long simulations allow electron density to reach the end of the volume and produce nonphysical reflections. To avoid artificial reflections from the boundaries during the time evolution, complex absorbing potentials (CAPs) are used near the boundaries. The CAP absorbs the outgoing waves and so prevents reflections from the boundaries. Figure 1 shows the arrangement of the system. The CAP is zero near the CN, and so does not impact current calculations. The CAP, taken from,²⁷ gradually increases to infinity at the right end of the simulation volume.

Previous time-dependent calculations^{23,24} first calculated the self-consistent Hamiltonian of the system, kept it constant, and time propagated the wave functions with that time-independent Hamiltonian. In this work, we solve the time-dependent Schrödinger equation by time propagating the wave function and the Hamiltonian in real time. The electronic density, the Hartree, and exchange-correlation potentials are updated at each time step. This fully time-dependent simulation approach describes, on an equal footing, the propagation of both the emitted electrons and the time-dependent charge redistribution on the nanotube in electric field. The unconditionally stable Crank-Nicolson²⁸ algorithm is used for the time propagation of the wave function

$$\Psi_k(\mathbf{r}, t + \Delta t) = \left(1 + \frac{i\Delta t}{\hbar} H\right)^{-1} \left(1 - \frac{i\Delta t}{\hbar} H\right) \Psi_k(\mathbf{r}, t). \quad (5)$$

The system's ground state is used for the initial state $\Psi(\mathbf{r}, t=0)$. The time-dependent Hamiltonian is the sum of the

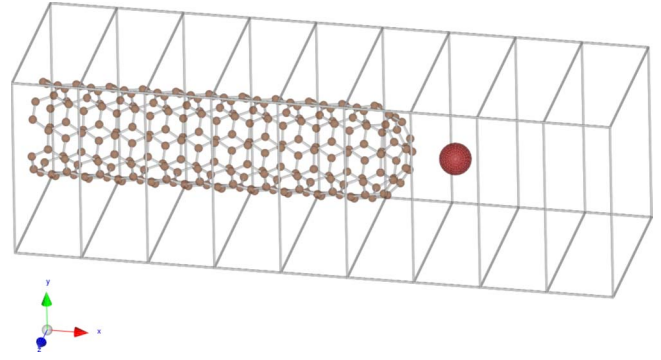


FIG. 2. (Color online) Decomposition of a tipped, capped (5,5) carbon nanotube into boxes.

Kohn-Sham Hamiltonian H_{KS} , the electric field $V_E = -eEx$, and the absorbing potentials W_L and W_R , $H = H_{KS}(t) + V_E + W_L + W_R$.

For wave function propagation, the most expensive numeric operations are products of the Hamiltonian matrix and the wave function. We use a multidomain decomposition to facilitate the efficient time propagation of the wave function. First, we divide the computational region into N boxes along the nanotube axis as shown in Fig. 2. The set of boxes is described by a basis function set ϕ_ν with $\nu = (ij)$ where i is the box index and j is the index of the basis function in a given box and $\Psi_k(\mathbf{r}, t) = \sum_\nu c_{\nu k}(t) \phi_\nu(\mathbf{r})$. The box basis functions are allowed to overlap with those in the neighboring boxes but only with the nearest neighbors. This causes the Hamiltonian and the overlap matrices of the system to be sparse structured block tridiagonal matrices. By exploiting the block tridiagonal structure of these matrices, the computational burden of the matrix multiplication and inversion steps of the Crank-Nicolson algorithm can be significantly reduced. This block tridiagonal algebra-based implementation allows the time-dependent simulation of large systems that would not be practical with conventional approaches. The time-dependent density-functional calculations presented here are implemented using our Lagrange function²⁹ based real-space real-time code.

III. NUMERICAL RESULTS AND DISCUSSION

In this section, we present our numerical calculations using a 20 Å long capped (5,5) carbon nanotube as a model system. To determine the position of the adsorbate, the adsorbate atom was positioned in front of the CN (see Fig. 1) and the system was relaxed by first-principles geometry optimization using the *ab initio* plane wave code VASP.³⁰ In these calculations, the atomic positions of the adsorbate atom and the carbon atoms forming the cap of the CN were allowed to relax while the rest of the system was kept fixed. Convergence was achieved when the forces on atoms were less than 0.05 eV Å. The obtained binding energies and bond distances (see Table I) are in good agreement with previous calculations.³¹ This static geometry optimization approach is a compromise dictated by computational limitations. In a more elaborate calculation, one would do a first-

TABLE I. Field-emission current for (5,5) capped nanotubes with various adsorbate atoms in a $1 \text{ V}/\text{\AA}$ electric field.

Adsorbate	Current (μA)	Tip distance (\AA)
None	28.4	
F	75.5	1.38
Cs	117.4	2.28
S	176.0	1.83
Al	189.3	2.21
Au	190.9	2.28
Ag	200.3	2.43
Si	216.6	2.02
W	276.4	2.12

principles molecular dynamics simulation in the presence of the electric field. But then, for a consistent description, one should account for the field emission of electrons during the molecular dynamics (picosecond time range) which is computationally unfeasible. One expects that in the presence of an electric field, the equilibrium position would be slightly different. We have shifted the adsorbates $\pm 0.1 \text{ \AA}$ from its equilibrium position to test the effect of the position change on the current. The current has changed by less than 10% due to the shift in position. While this shows the expected sensitivity of the field-emission current on the position of the adsorbate, the calculations show that the relative currents of various adsorbates remain similar.

Once the ground state of the system is calculated, the electric field is added and time development for 2 fs begins. The electric field's magnitude is increased slowly with a linear ramp over 0.2 fs. Once a steady state has been reached, the FE current is measured. The calculated currents for several adsorbates are given in Table I. The results show that compared to the untipped case almost an order of magnitude increase can be achieved by an adsorbate atom at $1 \text{ V}/\text{\AA}$, which is a typical electric field used in experiments. Calculations using different electric fields show a similar tendency (see Fig. 3). The calculated field enhancement factor for Cs

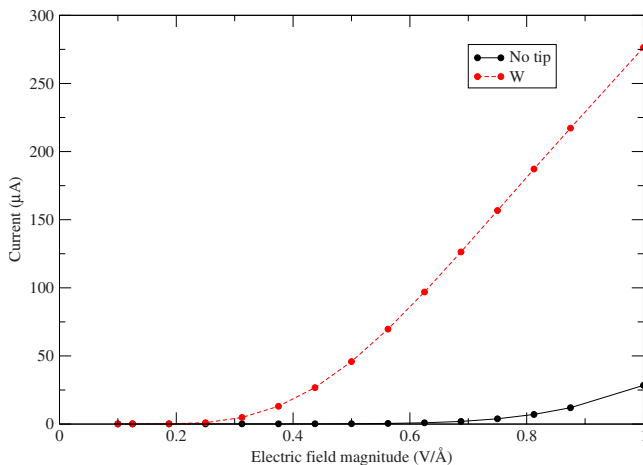


FIG. 3. (Color online) Current vs electric field magnitude for no tip and a W tip.

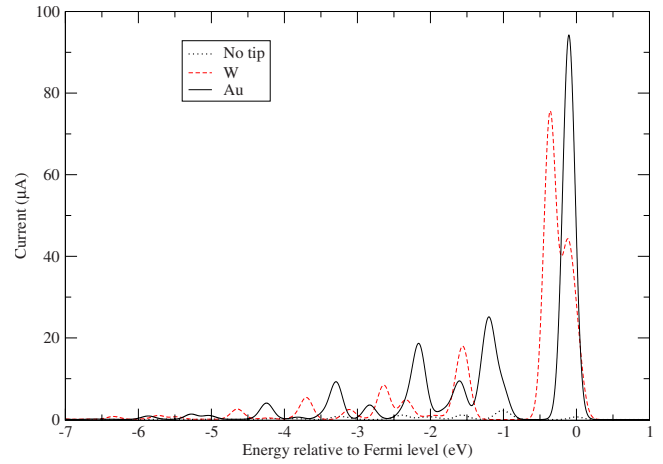


FIG. 4. (Color online) Current vs energy, relative to Fermi energy

is about 4, which is smaller than the experimentally observed order of magnitude increase,¹⁵ but it is in good agreement with the theoretical prediction of 3.4 in Ref. 32. The direct comparison to the experiment is difficult, because in the experiments (1) longer, thicker and most probably multiwall CNs are used and (2) several adsorbate atoms can be present in different cap positions. The addition of adsorbate atoms always increased the field-emission current. Some experiments show decrease in field-emission current in presence of CO , CO_2 , and CH_4 molecules.^{13,14} The study of the effect of molecules will be the subject of our subsequent work. The role of the adsorbate atom in the enhancement of the field-emission current is twofold. The calculations show that (1) the adsorbate atom lowers the potential energy barrier for the emitted electrons and (2) the adsorbate atom introduces extra electronic states at and above the HOMO in the CN spectrum. The energy spread of the emitted current is illustrated in Fig. 4. This energy spectrum shows that the majority of the field-emission current comes from states located near the Fermi energy. These states are introduced by the adsorbate atom and localized at the tip of the capped CN. When the electric field is turned on, these are the states that are propagated into the vacuum carrying the emitted current. These adsorbate-induced states, which do not exist in the case of the untipped CN, are the major contributors to the enhanced

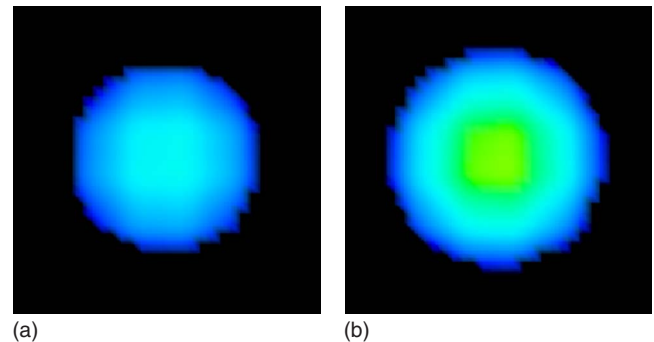


FIG. 5. (Color online) Two-dimensional spatial pattern of field-emission intensity at an electric field magnitude of $1.0 \text{ V}/\text{\AA}$, for various tips.

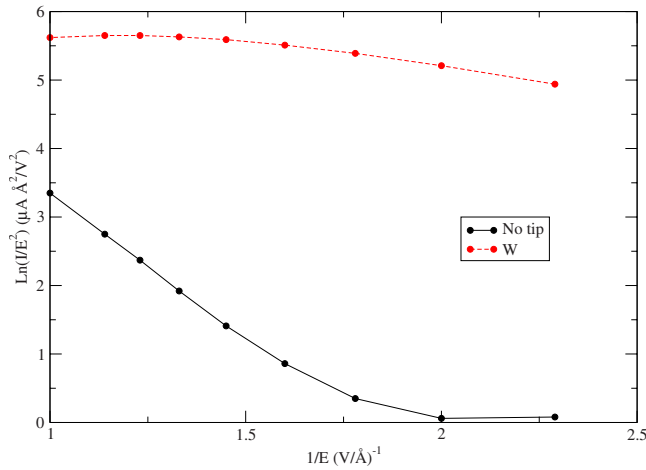


FIG. 6. (Color online) Fowler-Nordheim plot for no tip and a W tip.

current. Spatial snapshots of the emitted current are shown in Fig. 5.

Some experiments on CN field emitters show linear^{33,34} Fowler-Nordheim plots (at least in certain field regions) while others are nonlinear.^{35,36} Figure 6 shows the calculated Fowler-Nordheim plot for the untipped and W adsorbed CN.

Both the untipped and the W adsorbed CN Fowler-Nordheim plot are nonlinear and there is a large difference between the behavior of the two systems. The difference in behavior of W tipped and untipped CN clearly indicates the role of local fields and atomistic details in determining the field-emission properties of CNs. Direct qualitative comparison to experiment is difficult, because of the short length of the CN used in the calculation and the missing information on the chirality of the nanotubes used in the experiments.

In summary, the effect of adsorbates on the field-emission properties of CN are investigated using a real-space real-time TDDFT framework. Microscopic description of electron field emission from CN is presented. These studies are important for both understanding the fundamental physics of field emission from CN and future field-emission device applications. It is found that adsorbate atoms significantly increase the field-emission current. Adsorbate atoms also cause strong differences and nonlinearity in the Fowler-Nordheim plot. The source of the enhanced current is electronic states introduced by the adsorbate atom.

ACKNOWLEDGMENTS

This work is supported by NSF Grants No. ECCS0925422 and No. CMMI0927345.

- ¹W. de Heer, A. Châtelain, and D. Ugarte, *Science* **270**, 1179 (1995).
- ²Y. Saito *et al.*, *Nature (London)* **389**, 554 (1997).
- ³W. Choi *et al.*, *Appl. Phys. Lett.* **75**, 3129 (1999).
- ⁴A. Rinzler *et al.*, *Science* **269**, 1550 (1995).
- ⁵Y. Saito and S. Uemura, *Carbon* **38**, 169 (2000).
- ⁶K. A. Dean and B. R. Chalamala, *J. Appl. Phys.* **85**, 3832 (1999).
- ⁷N. de Jonge, Y. Lamy, K. Schoots, and T. Oosterkamp, *Nature (London)* **420**, 393 (2002).
- ⁸H. Schmid and H.-W. Fink, *Appl. Phys. Lett.* **70**, 2679 (1997).
- ⁹Y. Song, B. Usner, J. Choi, S. Lim, and Y. Lee, *Mater. Res. Soc. Symp. Proc.* **706**, 125 (2001).
- ¹⁰C. Dong and M. C. Gupta, *Appl. Phys. Lett.* **83**, 159 (2003).
- ¹¹K. A. Dean, P. von Allmen, and B. R. Chalamala, *J. Vac. Sci. Technol. B* **17**, 1959 (1999).
- ¹²K. A. Dean and B. R. Chalamala, *Appl. Phys. Lett.* **76**, 375 (2000).
- ¹³L. M. Sheng *et al.*, *J. Vac. Sci. Technol. A* **21**, 1202 (2003).
- ¹⁴K. Hata, A. Takakura, and Y. Saito, *Ultramicroscopy* **95**, 107 (2003).
- ¹⁵D.-H. Kim *et al.*, *Chem. Phys. Lett.* **355**, 53 (2002).
- ¹⁶A. Wadhawan, R. E. Stallcup II, and J. M. Perez, *Appl. Phys. Lett.* **78**, 108 (2001).
- ¹⁷E. Runge and E. K. U. Gross, *Phys. Rev. Lett.* **52**, 997 (1984).
- ¹⁸R. H. Fowler and L. Nordheim, *Proc. R. Soc. London, Ser. A* **119**, 173 (1928).
- ¹⁹K. L. Jensen, *J. Appl. Phys.* **85**, 2667 (1999).
- ²⁰N. D. Lang, A. Yacoby, and Y. Imry, *Phys. Rev. Lett.* **63**, 1499 (1989).
- ²¹Y. Gohda, Y. Nakamura, K. Watanabe, and S. Watanabe, *Phys. Rev. Lett.* **85**, 1750 (2000).
- ²²A. Maiti, J. Andzelm, N. Tanpipat, and P. von Allmen, *Phys. Rev. Lett.* **87**, 155502 (2001).
- ²³S. Han, M. H. Lee, and J. Ihm, *Phys. Rev. B* **65**, 085405 (2002).
- ²⁴K. Tada and K. Watanabe, *Phys. Rev. Lett.* **88**, 127601 (2002).
- ²⁵N. Troullier and J. L. Martins, *Phys. Rev. B* **43**, 1993 (1991).
- ²⁶E. K. U. Gross and W. Kohn, *Phys. Rev. Lett.* **55**, 2850 (1985).
- ²⁷D. E. Manolopoulos, *J. Chem. Phys.* **117**, 9552 (2002).
- ²⁸Edward A. McCullough, Jr. and R. E. Wyatt, *J. Chem. Phys.* **54**, 3578 (1971).
- ²⁹K. Varga, Z. Zhang, and S. T. Pantelides, *Phys. Rev. Lett.* **93**, 176403 (2004).
- ³⁰G. Kresse and J. Furthmüller, *Phys. Rev. B* **54**, 11169 (1996).
- ³¹E. Durgun, S. Dag, S. Ciraci, and O. Gulseren, *J. Phys. Chem. B* **108**, 575 (2004).
- ³²M. Khazaei and Y. Kawazoe, *Surf. Sci.* **601**, 1501 (2007).
- ³³D. Y. Zhong, G. Y. Zhang, S. Liu, T. Sakurai, and E. G. Wang, *Appl. Phys. Lett.* **80**, 506 (2002).
- ³⁴Q. H. Wang, T. D. Corrigan, J. Y. Dai, R. P. H. Chang, and A. R. Krauss, *Appl. Phys. Lett.* **70**, 3308 (1997).
- ³⁵L. H. Chan *et al.*, *Appl. Phys. Lett.* **82**, 4334 (2003).
- ³⁶P. G. Collins and A. Zettl, *Phys. Rev. B* **55**, 9391 (1997).